A MAGNETICALLY-SUSPENDED MIRROR DRIVING MECHANISM FOR FTIR

Hiroshi TAKAHASHI, Toshikatsu AKIBA and Fumika KONDO
Research and Development Center, Toshiba Corporation, Kawasaki, Japan
Kenichi TAKAHARA
Komukai Works, Toshiba Corporation, Kawasaki, Japan
Seizi NISHIZAWA and Kikuo SHIRAWACHI
Earth Observation Program, JASCO Corporation, Tokyo, Japan

ABSTRACT

The authors have developed a magnetically-suspended mirror driving mechanism for a greenhouse gas monitoring interferometer to be mounted on an airplane. An atmosphere observation program with the aim of global monitoring of greenhouse effect gasses such as CO_2 gas is being planned in Japan. The greenhouse gas monitor is based on a Fourier transform infrared spectrophotometer (FTIR) using a Michelson interferometer scheme. Therefore, the greenhouse gas monitor requires a linear driving mechanism. The magnetically-suspended mirror driving mechanism has such advantages as high pointing accuracy and vibration isolation, since it is driven without contact. According to the functional test results, this mechanism has been confirmed to have excellent performances. This paper presents the structure of the mechanism and the functional test results.

INTRODUCTION

The Earth's atmosphere contains CO_2 and many other ingredients which absorb outgoing infrared radiation from the Earth to space and warm the Earth's atmosphere, thus giving rise to the "greenhouse effect". Recent human activity increases such greenhouse gasses, and the increase in the temperature of the atmosphere is predicted to be 0.3 degrees. (Ref.[1]) Therefore, an atmosphere observation program with the aim of global monitoring of greenhouse effect gasses, is being planned in Japan.

The Advanced Earth Observation Satellite (ADEOS) will be launched for global observation of the Earth's environment in early 1996. It carries an interferometric monitor for greenhouse gasses (IMG). Observations from space yield information on the global atmosphere. IMG is a Fourier transform infrared spectrophotometer, and requires a mirror and a mirror linear driving mechanism for interferometry. In the IMG system, the mirror driving mechanism is a key part. One of the authors has already announced a mirror driving mechanism using a magnetic bearing for IMG. (Ref.[2]) This mechanism has long stroke and high pointing accuracy of the order of 0.0001 degrees. A magnetically-suspended mechanism has such advantages as high pointing accuracy, vibration isolation and mechanism reliability, since it is driven without contact. (Ref.[3]) Therefore, the magnetically-suspended linear driving mechanism is superior to other mechanisms using a ball screw type mechanism or a parallel spring type mechanism.

Furthermore, the authors have developed a magnetically-suspended mirror driving mechanism for a greenhouse gas monitoring interferometer which will be mounted on an airplane. Observation from airplanes, to verify observation data obtained from space by the satellite, is

TABLE 1: REQUIREMENTS

ITEMS	SPECIFICATION
DRIVING DISTANCE FOR DATA ACQUISITION	41.48mm
DRIVING RANGE	60mm
POINTING ACCURACY	
TRANSLATIONAL MOTION	±1.5micrometer
ROTATIONAL MOTION	±0.00097deg (±3.5 arcsec.)
LINEAR MOTOR FORCE	2.5N
MECHANISM	
WEIGHT	17kg
DIMENSIONS	230(W)×520(D)×220(H)mm
CONTROLLER	
WEIGHT	45kg
DIMENSIONS	800(W)×500(D)×300(H)mm
POWER CONSUMPTION	600W (AT DC) 100VA(AT AC100V)
THERMAL ENVIRONMENT	10 to 30℃
VIBRATION ENVIRONMENT	1.3mG

also planned in Japan. (Ref. [4]) The mirror driving mechanism equipped on the airplane must be capable of maintaining the required pointing accuracy when suspended and driven under the vibration environment of the airplane.

DESIGN DESCRIPTION

REQUIREMENTS

The FTIR requires the mirror driving mechanism to have a long stroke and high pointing accuracy. The required specifications for the FTIR are shown in Table 1. The main requirements are as follows.

(1)The driving mirror (corner cube mirror) should be controlled with an excellent pointing accuracy of ±1.5 micrometers for translational motions and ±0.00097 degrees for rotational motions.
(2)The driving distance for interferogram data acquisition is 41.48 mm, so the linear driving range is 60 mm long.
(3)The driving speed is 26 mm/sec at a driving distance of 41.48 mm. Thus, the driving force for the linear motor is more than 2.5 N.

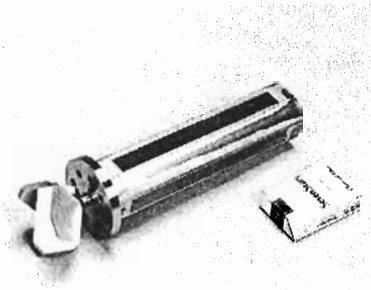

FIGURE 1: DRIVING SHAFT

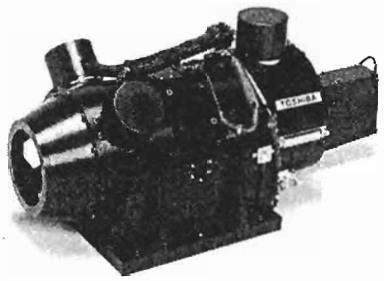

FIGURE 2: MECHANISM

(4)The FTIR is able to satisfy the performance goals under a vibration environment on the airplane of max. 1.3 mG.
(5)The mechanism weight is less than 17 kg, and the controller weight is less than 45 kg.

MECHANISM

Figure 1 shows a photograph of the corner cube mirror which is fixed to the driving shaft, and Fig. 2 shows the newly developed mechanism. This mechanism mainly consists of a driving shaft made of a ferromagnetic material, a corner cube mirror mounted on the driving shaft, 8 horseshoe shape electromagnets, 8 eddy current type displacement sensors for magnetic bearing control, a voice coil type linear motor, a laser beam linear position sensor for linear driving control, 3 shaft lock devices, a hollow cylindrical housing, and a base. Fig. 3 shows a cross sectional view. This mechanism has 4 degrees of freedom, that is, 2 translational and 2 rotational motions controlled by the 8 electromagnets. The driving shaft motion along the linear driving axis is controlled by the linear motor. The driving shaft rotation around the linear driving axis is passively stabilized.

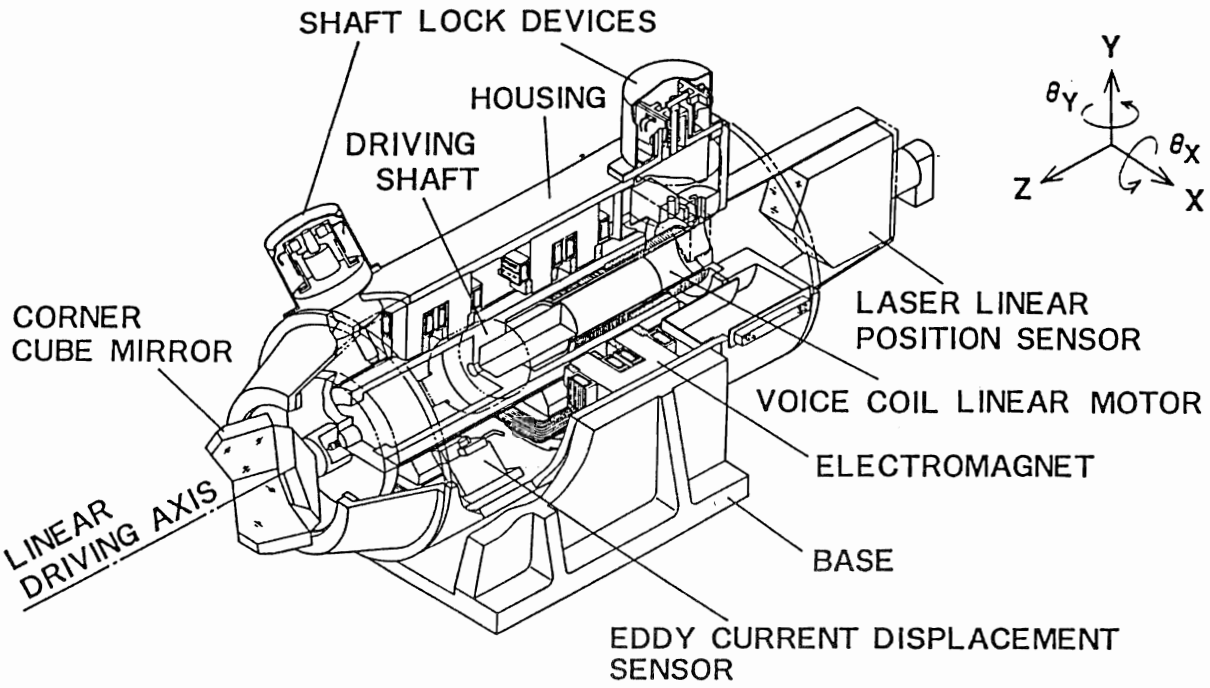

FIGURE 3: STRUCTURE OF MECHANISM

The targets of displacement sensors are the key point of the mechanical design for the linear driving mechanism. The displacement sensor targets on the driving shaft are used for detecting the driving shaft position. These displacement sensor targets are separated from the magnetic pole of the electromagnets. Therefore, the displacement sensor targets are not influenced by the magnetic field. The targets are made flat on an order of 0.1 micrometer within the driving range for the high pointing control.

The linear motor consists of a motor coil and a permanent magnet. The important feature of this linear motor is that it has no mechanical contact drive. Generally, a voice coil type linear motor uses a moving coil drive, since a moving magnet type linear motor does not have a good dynamic response. Because a long driving range is necessary, the permanent magnet which is mounted on the driving shaft in the moving magnet type linear motor, is heavy and large. However, the moving magnet type linear motor for this mechanism is compact and lightweight, since the design is optimized for magnetic field analysis. A short permanent magnet is inserted into the driving shaft and a long motor coil is attached in the housing, and the motor coil is interposed

TABLE 2: SPECIFICATIONS OF MECHANICAL DESIGN

ITEMS	SPECIFICATION
[DRIVING SHAFT]	
PAYLOAD	CORNER CUBE MIRROR
WEIGHT	3.7kg(INCLUDING MIRROR)
MOMENT OF INERTIA	
DRIVING AXIS	$0.0013 kgm^2$
RADIAL AXIS	$0.0199 kgm^2$
[MAGNETIC BEARINGS]	
DEGREES OF FREEDOM	4(CONTROLLED)
ELECTROMAGNETS	
NUMBER	8
SHAPE	HORSESHOE SHAPE
PULL FORCE	18.6N (AT 0.5mm AIR GAP,1A)
DISP.SENSORS	
NUMBER	8
TYPE	EDDY CURRENT SENSOR
MEASURING RANGE	2mm
[LINEAR MOTOR]	
TYPE	VOICE COIL TYPE
DRIVING RANGE	60mm
MAX. DRIVING FORCE	> 6.7N(AT 2A)
[SHAFT LOCK DEVICES]	
NUMBER	3
TYPE	SOLENOID

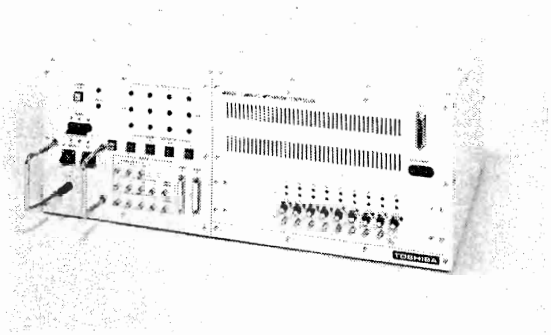

FIGURE 4: CONTROLLER

in the driving shaft. The permanent magnetic flux for the linear motor passes down the working air gap, axially along the driving shaft, then returns to the permanent magnet. The electromagnetic flux in the air gap for the magnetic bearing receives no influence from the permanent magnetic flux in the linear motor, because the electromagnetic flux circuits are closed locally. The permanent magnetic flux that passes the air gap in the electromagnet circuit, is almost zero.

The specifications of the mechanical design parameters are shown in Table 2.

CONTROLLER

Fig. 4 shows a photograph of the controller. In this magnetic bearing control, each electromagnet is independently controlled by an individual analog PID compensator in the local electromagnet coordinate system. The displacement between the driving shaft and the displacement sensor is detected by each displacement sensor. These sensor signals are transformed into the displacement signal of the force operating point in the electromagnet position, since the sensors are not collocated with the electromagnets. The sensor signals are fedback to the PID compensator. The position compensator adjusts a radial position of the driving shaft to realize a high pointing accuracy during the driving shaft long stroke motion under gravity.

STIFFNESS AND STABILITY OF BEARINGS

Fig. 5 shows the relationship between the natural frequency and the bearing stiffness. The bearing stiffness is

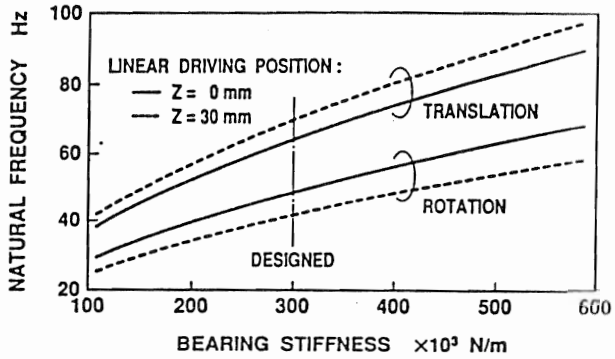

FIGURE 5: NATURAL FREQUENCY

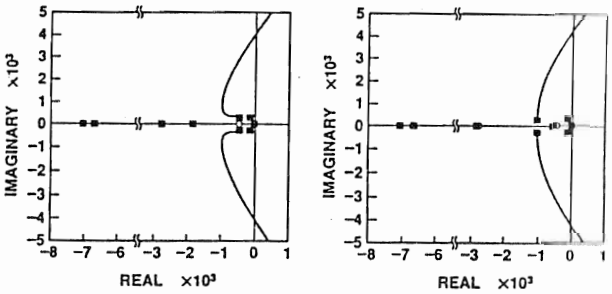

a) SHAFT POSITION Z=0 mm b) SHAFT POSITION Z=30 mm

FIGURE 6:ROOT LOCI OF MAGNETIC BEARING CONTRCL SYSTEM FOR TRANSLATIONAL MOTION

designed to be 300 N/mm, because the natural frequency for the magnetic bearing does not agree with the vibration frequency on the airplane, in any position of the linear driving shaft.

Fig. 6 shows the root loci of the magnetic bearing control system for translational motion in the cases when the shaft position Z=0 mm and Z=30 mm. In the figure, the shaft position Z=0 mm indicates the middle point of the right and left side bearing. According to these figures, the calculation results indicate that the controller has sufficient ability to stabilize the driving shaft even when the shaft position is Z=30 mm at the end of the driving stroke.

EXPERIMENTAL RESULTS

DYNAMIC CHARACTERISTICS OF BEARINGS

Fig. 7 shows the relationship between the resonance frequency and the linear driving position in the magnetic bearing. The resonance frequency of the magnetic bearing and vibration frequency on the airplane should not agree, in order to ensure the required pointing accuracy under the vibration environment of an

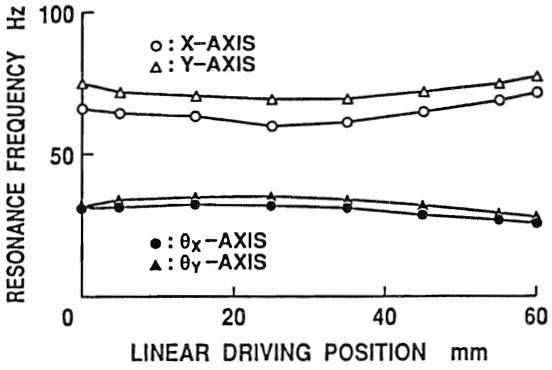

FIGURE 7: RESONANCE FREQUENCY

airplane. The vibration frequencies measured on the airplane are mainly 33 Hz, 65 Hz and 98 Hz. The vibration frequencies 33 Hz and 98 Hz influence translational motion control of the magnetic bearing, and 65 Hz and 98 Hz influence rotational motion control. However, the vibration influence is small even when driving the shaft for a long stroke, because, the resonance frequency of the magnetic bearing has been confirmed to be about 70 Hz in the translations and about 30 Hz in the rotations.

POINTING ACCURACY

When driving the mirror along the Z axis, the pointing error during the linear driving motion was independently determined in each way. This is called pointing accuracy. The pointing accuracy for translational motion is shown in Fig. 8. Similarly, Fig. 9 shows the pointing accuracy for rotational motion. These pointing results confirm that the pointing accuracy for translation is ±0.6 micrometers on the X-axis and ±0.8 micrometers on the Y-axis. Similarly, the pointing accuracy for rotation was confirmed to be ±0.0003 degrees on both the θ_X-axis and θ_Y-axis. This pointing error is mainly caused by the displacement sensor target flatness within the driving range and the gravity influence. These test results are shown in Table 3.

Table 4 shows test results of the pointing error in a disturbed environment. This environment was created in the authors' laboratory and was equivalent to the disturbed environment on an airplane. This mechanism has realized a high pointing accuracy in spite of the driving shaft long stroke motion under the environment simulating the vibration of an airplane.

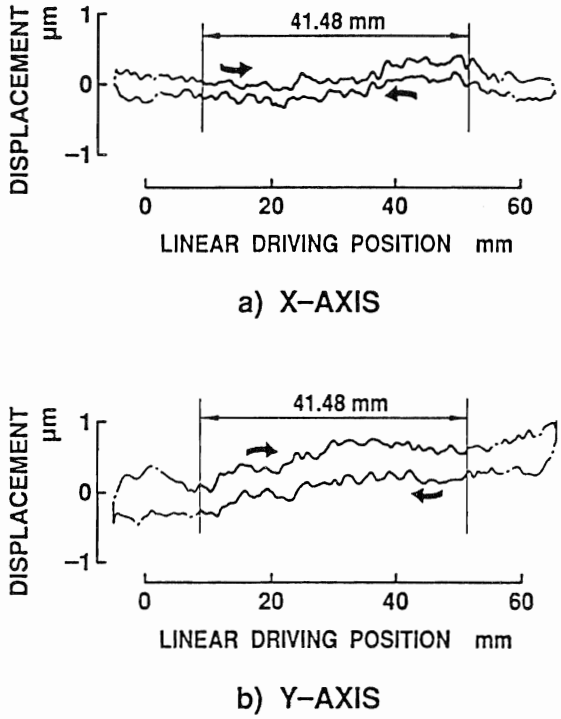

FIGURE 8: POINTING ACCURACY FOR TRANSLATIONAL MOTION

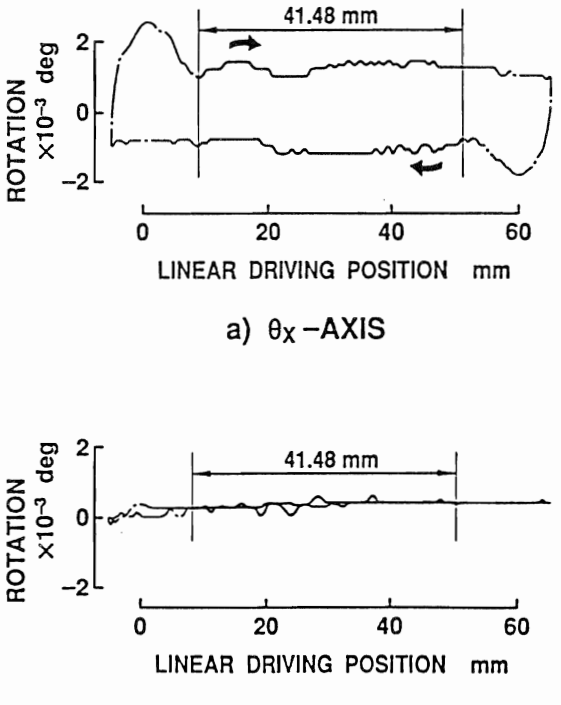

FIGURE 9: POINTING ACCURACY FOR ROTATIONAL MOTION

TABLE 3: POINTING ACCURACY

ITEMS	PERFORMANCE
TRANSLATIONAL MOTION	X-AXIS :±0.6micrometer
	Y-AXIS :±0.8micrometer
ROTATIONAL MOTION	θ_X-AXIS:±0.0003deg
	θ_Y-AXIS:±0.0003deg

TABLE 4: POINTING ERROR WITH DISTURBANCE

ITEMS	PERFORMANCE
TRANSLATIONAL MOTION	X-AXIS :±0.8micrometer
	Y-AXIS :±1.0micrometer
ROTATIONAL MOTION	θ_X-AXIS:±0.0006deg
	θ_Y-AXIS:±0.0005deg

LINEAR DRIVING FORCE

Fig.10 shows the permanent magnetic flux density of the driving shaft for the linear motor, and the static driving force is shown in Fig.11. Fig.11 is a graph showing plotted linear driving positions from 0 mm to 60 mm at 5 mm intervals. Since the leak flux of the permanent magnet has little influence on the linear motor, the driving force drops slightly when the coil current is +2 A and the linear driving position is 0 mm. However, the linear motor is confirmed to have a maximum driving force of ±6.7 N, which is more than the required driving force ±2.5 N.

CONCLUSIONS

The authors have developed a magnetically-suspended mirror driving mechanism for a greenhouse gas monitoring interferometer on an airplane. In the authors' laboratory, the mechanism has been confirmed to have a pointing accuracy of ±0.8 micrometers for translational motions and ±0.0003 degrees for rotational motions. According to the test results, this mechanism has realized a high pointing accuracy in spite of the driving shaft long stroke motion under gravity and simulated vibration environment of an airplane. Therefore, this mechanism for FTIR is clearly superior to other mechanical linear driving mechanisms.

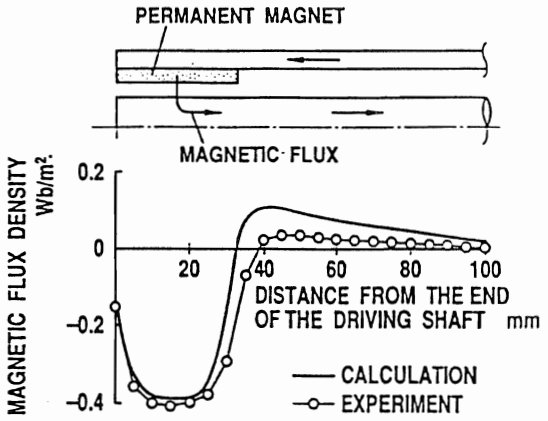

FIGURE 10: MAGNETIC FLUX DENSITY OF DRIVING SHAFT FOR LINEAR MOTOR

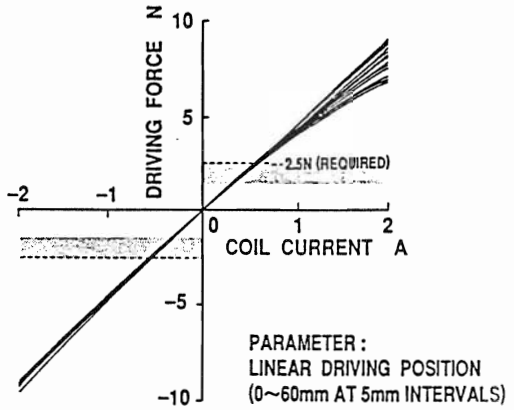

FIGURE 11: STATIC CHARACTERISTICS OF LINEAR MOTOR

REFERENCES

[1]K.Tsuno, et al., Interferometric monitor for greenhouse gasses for ADEOS, SPIE Vol.1490 Future European and Japanese Remote-Sensing Sensors and programs, 1991

[2]T.Akiba, et al., Development of a Magnetically-Suspended Mirror Scanning Mechanism for an Interferometric Monitor for Greenhouse Gasses(IMG), Proceedings of 3rd International Symposium on Magnetic Bearings, 73-82, Virginia, 1992

[3]H.Takahashi, et al., Development of a Magnetically-Suspended Antenna Pointing Mechanism (System Recovery in Case of Electromagnet/Sensor Damage in a Redundant System), Proceedings of 3rd International Symposium on Magnetic Bearings, 91-100, Virginia, 1992

[4]H.Kobayashi, et al., Design Status of the Airborne FTIR for IMG Data Retrieval, Proceedings of the 4th International Symposium on Atmospheric Science from Space using FTS, 1993